# PROCESS MODELLING, SIMULATION AND EXPERIMENTAL VALIDATION FOR PREDICTION OF CHIP MORPHOLOGY DURING HIGH SPEED MACHINING OF AL 2024-T3

**Arvind Jeevannavar, *Raja Hussain**

Mechanical and Manufacturing Engineering, M. S. Ramaiah School of Advanced Studies, Bangalore 560 054

*Contact Author e-mail: Hussain.sm5@gmail.com

## *Abstract*

*Metal cutting is one of the most widely used manufacturing techniques in the industry and there are lots of studies to investigate this complex process in both academic and industrial world. Predictions of important process variables such as cutting speed, cutting feed and stress distributions play significant role on validating chip morphology. Researchers find these variables by using experimental techniques which makes the investigation very time consuming and expensive. At this point, finite element modelling and simulation becomes main tool. These important cutting variables can be predicted without doing any experiment with finite element method.*

*The aim of this project is to create a numerical model to examine the chip morphology convinced by orthogonal machining in the finished work piece and the chip is validated by numerical simulation comparing with experimental result. The Finite Element Method (FEM) is used to simulate and compare chip morphology with experimental result which is simulated by an orthogonal metal cutting process. Therefore, Arbitrary Langrangian-Eulerian (ALE) adaptive meshing Finite Element Method (FEM) is employed to simulate the model. The Johnson-Cook material model is used to describe the work material behavior and fully coupled thermal-stress analysis are combined to realistically simulate high speed machining with an orthogonal cutting.*

*Therefore, orthogonal cutting simulations of Al2024-T3 are performed and simulated result along with experimental is validated. In first step, effects of work piece flow stress and friction models on cutting variables such as chip geometry is investigated by comparing simulation results with experimental results available in the literature. Chip morphology study is understood by validating the chip width and chip thickness based on numerical validation with experimental result and also agreed that numerical simulation is important tool to predict chip morphology, chip formation without carrying lots of trial and error activity on machine shop which is really necessary for today's competitive market.*

**Key Words: Abaqus, FEM, Chip morphology, Orthogonal metal cutting.**

**Nomenclature**

| | |
|---|---|
| ALE | - Arbitrary Lagrangian-Eulerian |
| CAE | - Computer Aided Engineering |
| FEM | - Finite Element Method |
| FEA | - Finite Element Analysis |
| HSM | - High Speed Machining |
| J-C | - Johnson Cook |

## 1. INTRODUCTION

Machining is the process of removing the material in the form of chips by means of wedge shaped tool. The most common manufacturing process in industry is cutting, and FEM (Finite Element Method) has become the main tool for simulating metal cutting processes. The depth of cut is the movement between work piece and the cutting tool, which determines the thickness of material to be removed. The chip can be continuous, segmented, or discontinuous; depending on the cutting parameters applied. Temperature also affects tool life, work piece surface finish, chip morphology, and power consumption.

The complexity of chip formation in machining processes stems from the confluence of several physical phenomena - mechanical, thermal, and chemical - occurring at very high strain rate. The prediction of chip morphology depends on a fundamental understanding of these phenomena and is of industrial importance for cutting force prediction and surface integrity control. Thesis study is on characterizing the chip morphology and discusses the physical phenomena associated chip formation according to finite element modelling (FEM) simulations. Selection of cutting parameters directly influences the interaction at the tool-chip interface and consequently the chip morphology. This is especially true with the complex tool geometries currently in use on the market. Moreover, the tool-chip interface is the excitation element for the dynamic behavior of the machining system, i.e. these interactions affect the dynamics of the cutting process. Computer simulations of the cutting process complement the experimental approach by minimizing the number of design iterations and reducing design cost. Unfortunately, few valid physics-based models are available due to the high strain rate of chip formation and the mechanical, thermal, and metallurgical complexity of the tool-work piece interactions. Due to increasing interest in high-speed machining, investigations of chip formation with

high cutting speeds and hard materials have appeared. Thus, cutting speed has been the primary parameter studied for chip formation simulation. Few numerical studies have been made concerning the chip formation according to feed rate [1].

## 2. LITERATURE REVIEW

Chip formation and its morphology are the key areas in the study of machining process that provide significant information on the cutting process itself. The chip morphology depends upon the work piece material properties and the cutting conditions. The main chip morphologies observed in cutting process are the continuous and the cyclic or serrated chips. Finite element simulations are considered a widespread and strong tool in the study of metal cutting. Due to its comprehensive ability, finite element simulations take into account large complexities that come upon metal cutting. However, over the last 20 years, developments in technology (hardware and FE codes) dramatically increased, overcoming to an extent the limitations faced in modelling and computational difficulties. Commercially available software packages became more in use [2, 3]. These packages included NIKE-2D, DEFORM, FORGE2D, ABAQUS/standard, ABAQUS/Explicit, ANSYS/LS-DYNA, ALGOR and FLUENT.

Shih [4] developed a model to analyse the orthogonal metal cutting with continuous chip formation, using a Eulerian description. Shih found that the lack of complete material properties and friction parameters directly impacts the accuracy of the finite element simulation. Also, Shih [5] studied the effect of the rake angle in the cutting processes. In his doctoral thesis, Kalhori [6] investigated different modelling approaches for the chip separation. The physical model of chip separation was found to be more suitable in simulation.

Stevenson, Wrigt and Chow [7] developed the finite element program for calculating the temperature distribution in the chip and tool in metal cutting. They compared the temperatures estimated with the temperatures obtained with previously described metallographic method. Stevenson has assumed the form of the chip and cutting tool initially and then obtained the required parameters from the simulation without simulating the separation of the chip for this current cutting condition. The needed data for simulation were obtained from experimental and theoretical results such as chip form.

Iwata, Osakada and Terasaka [8] developed a rigid-plastic finite element model for orthogonal cutting in a steady state condition. The methods for determining the material and frictional properties to be used in the model are discussed. The shape of chip and distributions of stress and strain are calculated. Fracture of chip is predicted by combining the present model with the criteria of ductile fracture. In this work, an initial model is generated by giving the cutting condition and the shape of the cutting tool, and then the model is modified by using the result of the plane strain finite element analysis.

Komvopoulos and Erpenbeck [9] modelled orthogonal chip formation process by using finite element method. They analyzed the effect of important factors, such as plastic flow of the work piece material, friction at the tool-work piece interface and wear of the tool on the cutting process. To simulate separation of chip from the work piece, distance tolerance criterion was used by super positioning two nodes at each nodal location of a parting line of the initial mesh. Elastic - perfectly plastic and elastic plastic with isotropic strain hardening and strain rate sensitivity constitutive laws was used in the analysis. For simplicity, the tool material and the built-up edge were modelled as perfectly rigid. Steady state magnitudes of the cutting force, shear plane angle, chip thickness and chip-tool contact length are estimated.

## 3. PROBLEM DEFINITION:

In recent years, the application of Finite Element Method (FEM) in cutting operations is one of the effective ways to study the cutting process and chip formation. In particularly, the simulation results could be used as a practical tool, both for researchers and tool makers to design new tools and to compare results with obtained experimental result. Facing in metal cutting of high speed machining process, it is very complicated to determine the optimization of cutting conditions due to a lot of cutting experiments need to be execute. Moreover, these experimental also consider in risks condition because not all the results from the experiments could be achieved as desired. For the results which are not fulfil the optimized cutting condition, the experiments should be repeated and this will lead to high costing to the industry manufacturer worldwide in terms of time demanding, human energy and work material respectively. In order to reduce the costs and time, Finite Element Method (FEM) in machining is widely used nowadays and has become main tool for simulating metal cutting process. Based on cutting experiments, the numerical simulation are carried out to verify using FEM to indicate that the simulation result are consistent or not with the experiments. This study aims to simulate cutting operations for understand chip morphology and compare with experimental obtained result and therefore FEM software used for this study is ABAQUS/Explicit.

### 3.1 Methodology

Literature(s) reviewed on Numerical Modelling for machining of Al2024-T3 alloy, cutting forces, cutting tool insert and process parameters for HSM and those are carried out by referring different journal papers, books, manuals and other related documents. Collected the cutting tool parameters and machining parameters like cutting speed, cutting feed and different depth of cut for an Al2024-T3 alloy from the selected literatures. Simulation tool ABAQUS/Explicit V6.10 is learnt to model 2D geometrical models of cutting tool and work-piece in ABABQUS / CAE for FEA numerical simulation prospective. Understand and studied Johnson-Cook material model which is used to describe the work material behavior. Range of spindle speeds, cutting feeds, tool rake angles and depth of cuts are selected and based on those; numerical trials are carried out using ABAQUS/Explicit commercial numerical

simulation software. After all numerical trials are runs those are investigated and measured numerically with respect to obtained chip width and chip thickness for all 9 different cases and of course those compared with obtained experimental result from machine shop. Finally, validation of the process is carried out.

## 4. NUMERICAL SIMULATION:

Understanding of the material removal process in metal cutting is important in selecting tool material and design and in assuring consistent dimensional accuracy and surface integrity of the ¬finished product, especially in automated production and precision parts manufacturing. Metal cutting is a highly nonlinear and coupled thermo-mechanical process, where the coupling is introduced through localized heating and temperature rise in the work piece, which is caused by the rapid plastic flow in the work piece and by the friction along the tool–chip interface. In recent years, finite element method became the main tool for the analysis of metal cutting. Because it has important advantages, which can be counted as follows.

- Material properties can be handled as a function of strain, strain-rate, and temperature.
- Nonlinear geometric boundaries, such as free surfaces, can be modelled.
- Other than global variables like cutting force, thrust force; local variables like strains, strain-rates, stresses, etc. can be obtained
- Interaction of chip and tool can be modelled in different forms.

### 4.1 Tool modeling

From the practical experience, it is proved that the tool geometry has a great influence on the surface geometry of the machined work piece, so it has been very keen importance in the model to design to tool geometry. From the practical experience, it is proved that the tool geometry has a great influence on the surface geometry of the machined work piece, so it has been very keen importance in the model to design to tool geometry. In the numerical simulation analysis, the tool is selected to be of Tungsten carbide (WC) material. The tool geometry (Figure 1) and work-piece material physical property data are listed in Table 1 and 2.

**Table 1. Geometric variables of cutting tool**

| Rake angle, α (°) | Clearance angle c (°) | Tool Nose Radius (mm) |
|---|---|---|
| 0° | +10° | 0.8mm |

**Table 2. Tool and work-piece property data**

| *Physical parameters* | *Tool* | Work piece |
|---|---|---|
| Density, ρ (Kg/m3) | 11900 | 2700 |
| Elastic modulus, E (Gpa) | 534 | 73 |
| Poisson's ratio, ν | 0.22 | 0.33 |
| Specific heat, (kJ/kg-K)) | 0.198 | 0.889 |
| Young's Modulus (Mpa) | 90000 | 70000 |
| $T_i$ (°C) | 25 | 25 |

### 4.2 Work-piece modeling

In the analysis, Al2024-T3 is selected as work piece material. Johnson-Cook (J-C) material constitutive models with properties as shown in table 3 are used to model the plastic behavior of Al2024-T3. In the ABAQUS numerical simulation, 2D geometrical model of work piece per dimension of 10mm x 5mm has been modelled and width of tool is considered as 1mm which is represented in ABAQUS as plane stress/strain thickness. In Figure 2, tool contacting face has been meshed very fine to obtain better simulation result and to reduce meshing computation time. As per presented in the figure A, B, C and D are meshed very fine and remaining portion the part not considered because tool only interface on ABCD deformation zone.

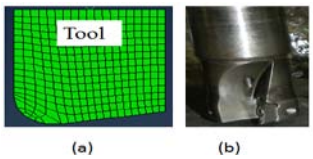


**Fig. 1 (a) 2D view Cutting tool (b) Cutting tool inserted in cutting tool holder**

**Table 3. J-C constants for model Al2024-T3**

| A | B | *n* | C | *m* | *α* | *c* |
|---|---|---|---|---|---|---|
| 369 | 684 | 0.73 | 0.0083 | 1.7 | 0° | 10° |

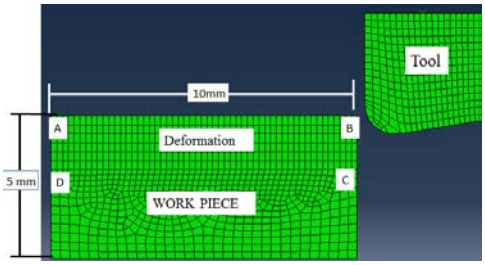


**Fig. 2 FEM simulations model for ALE formulation with fine mesh**

### 4.3 Element type

Since high speed machining involve non-linear, high temperature, high complexity of the machining operation, therefore, from numerical modelling point of view, it is very necessary to select the right element type for the FE-modelling, to handle this type of complex thermal-mechanical coupled problem, whereas large deformation are also the important factor. Hence, in this study, 4 node quadrilateral coupled temperature-displacement plain strain reduced integration elements CPE4RT (Figure 3) with ALE formulation is used to handle thermo-mechanical coupled machining problems.

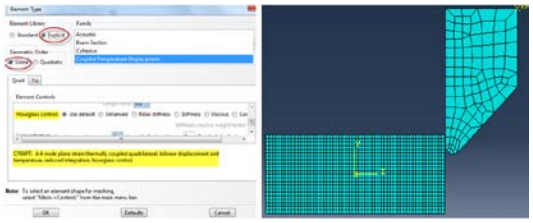

**Fig. 3 CPE4RT element screenshot from ABAQUS**

### 4.4 Tool-Chip Interface

The friction at the tool chip interface (Figure 4) is an essential element for understanding the system that forms the chip, but Friction in metal cutting is difficult to determine. Friction along with the tool-chip during cutting process is a very complex phenomenon. The friction influences the chip formation, built-up edge formation, cutting temperature and tool wear. Therefore it is necessary to understand the friction mechanism across the faces and around the tool edge, in order to be able to develop accurate models for cutting forces and temperature. During analysis, it is assumed that work piece does not undergo elastic deformation and it is allowed to show only plastic behavior. In the simulation model surface-to-surface contact conditions is used to define the tool-chip as well as tool-work piece contact pair. At this point numerical methods become important. In last two decades, finite element method (FEM) has been most frequently used in metal cutting analysis. Various outputs and characteristics of the metal cutting processes such as cutting forces, stresses, temperatures, chip shape, etc. can be predicted by using FEM without doing any experiment.

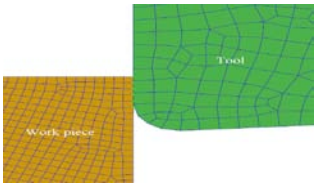


**Fig. 4 Contact generation between tool and work piece**

Dimensional model of the orthogonal metal cutting with plane strain assumption was developed in Abaqus FEA software. Before getting into the details of the modelling it is necessary to look into the assumptions made for the study to match the actual experiments carried out at Searock Precision Product Pvt Ltd industry and others to reduce the runtime without sacrificing the validity of the model. The assumptions are as follows:

1. The cutting takes place at a different spindle speed of 9000rpm,10000rpm and 11000 rpm respectively
2. The nose radius of the tool is constant at 0.8mm.
3. Tool is modeled as rigid and tool wear is neglected in this study to reduce the complexity and runtime.
4. Room temperature is assumed to be 25°C
5. A dry machining condition is considered for this simulation.
6. Homogenous material conditions are used.
7. Metric system of units (Kg, M, s, °C, N) is followed through the entire model.

The entire modelling and solving of the model can be classified into three distinct sections as Pre processing, Solving and post processing. The pre processing step involves the geometry modelling, material definition, boundary condition definition and discretization (meshing) which is then submitted to a solver which computes and outputs a set of numbers which is interpreted using the post processor. Post processor also helps in plotting different distributions and parameters with respect to time.

There are 9 different test cases (Figure 5) have been taken to predict chip morphology, chip thickness, chip width study, which are tabulated as per Table 4.

9 different simulations are modelled separately for each of the combinations mentioned above are built in the pre-processor and were saved as key cae file (.cae file) and those all 9 cases were given to run in Abaqus solver to get post processor result as shown in Figures 7 – 16. That being said, these .cae files were translated to .odb file as output file to view the simulation result to the solver running on the super computer to obtain the results.

**Table 4. Different test cases used in simualtion**

| Parameters | Test 1 | Test 2 | Test 3 | Test 4 | Test 5 | Test 6 | Test 7 | Test 8 | Test 9 |
|---|---|---|---|---|---|---|---|---|---|
| Spindle speed in rpm | 9000 | 10000 | 11000 | 9000 | 10000 | 11000 | 9000 | 10000 | 11000 |
| Depth of cut in mm | 0.5 | 0.5 | 0.5 | 1.0 | 1.0 | 1.0 | 1.5 | 1.5 | 1.5 |
| Tool Rake angle α in degree | 0° | 0° | 0° | 0° | 0° | 0° | 0° | 0° | 0° |
| Tool clearance angle in degree | +10° | +10° | +10° | +10° | +10° | +10° | +10° | +10° | +10° |
| Tool nose radius in mm | 0.8 | 0.8 | 0.8 | 0.8 | 0.8 | 0.8 | 0.8 | 0.8 | 0.8 |

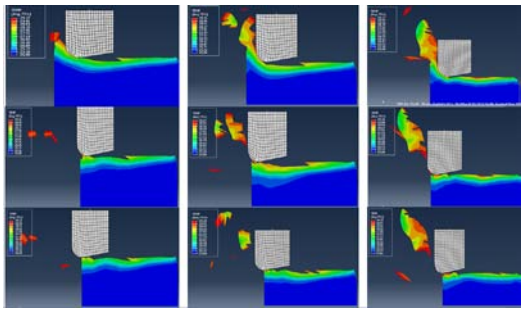

**Fig. 5 Different parameter simulations cases for chip formation in Al2024-T3 machining**

In Figure 6, chip simulation figure of Al2024-T3 at different spindle speed. As can be seen, in every simulation type of chip shape form changes slightly but chip type will continous type. As the cutting velocity increase, the cutting temperature on tool and work piece increases and cutting shape will be slighlty changes as per Figure 6.

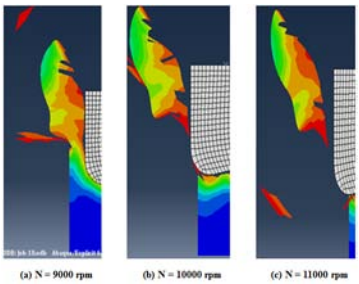


**Fig. 6 Chip figures at different spindle speed of 9000, 10000, 11000rpm respectively**

## 5. EXPERIMENTAL STUDIES:

The purpose of the experiments performed in this work is to verify the results of numerical solution obtained by the finite element method. During experiment, chip morphology study, validate and

measure to compare with numerical simulation. In addition, for every experiment, sample chips were collected and their thicknesses and chip width are measured with the help of digital caliper instrument in machine shop. Therefore, chip thickness, chip width as well as chip morphology from the experimental obtained work is compared with the numerical solutions by finite element method. Experiments are carried-out in *Searock Precision Products Pvt Ltd.* Different tests are carried out on Al2024-T3 alloy rectangular work piece dimension of 140mm x 140mm x 40mm and parametric model has been used as it has some advantages. Within the limitations of the range of cutting data, cutting geometry and work and tool material as shown in Table 5 it is quite accurate.

**Table 5. Work-piece and Tool properties used in machine shop**

| Material | Al2024-T3 |
|---|---|
| Dimension | 140mmX 40mmX80mm |
| Cutter Dia | 32mm |
| Cutter nose | 0.8mm |
| Rake angle | 0° |
| Relief angle | +10° |
| Cutter holder | BT 40 with 3 tips cutter |
| Cutting tool made | Tungsten carbide |

**Table 6. Cutting Conditions**

| Parameters | Test 1 | Test 2 | Test 3 | Test 4 | Test 5 | Test 6 | Test 7 | Test 8 | Test 9 |
|---|---|---|---|---|---|---|---|---|---|
| Spindle speed in rpm | 9000 | 10000 | 11000 | 9000 | 10000 | 11000 | 9000 | 10000 | 11000 |
| Depth of Cut in mm | 0.5 | 0.5 | 0.5 | 1.0 | 1.0 | 1.0 | 1.5 | 1.5 | 1.5 |
| Tool Rake angle α in degree | 0° | 0° | 0° | 0° | 0° | 0° | 0° | 0° | 0° |
| Tool clearance angle in degree | +10° | +10° | +10° | +10° | +10° | +10° | +10° | +10° | +10° |
| Tool nose radius (mm) | 0.8 | 0.8 | 0.8 | 0.8 | 0.8 | 0.8 | 0.8 | 0.8 | 0.8 |


**Fig. 7 Set-up for chip morphology study on experimental result**

**Fig. 8 DOC=0.5mm, Vc=900 m/min result**

**Fig. 9 DOC=0.5mm, Vc=1000 m/min result**

**Fig. 10 DOC=0.5mm, Vc=1100 m/min result**

**Fig. 11 DOC=1.5mm,Vc=900 m/min result**

**Fig. 12 DOC=1.5mm, Vc=1000 m/min result**

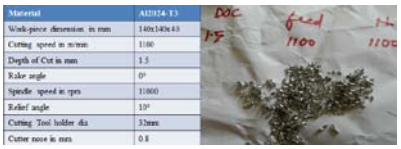

**Fig. 13 DOC=1.5mm, Vc=1100 m/min result**

**Fig. 14 DOC=1.0mm, Vc=900 m/min result**

**Fig. 15 DOC=1.0mm, Vc=1000 m/min result**

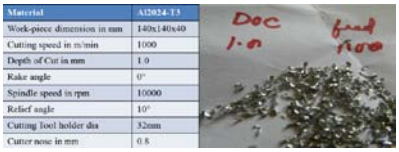

**Fig. 16 DOC=1.0mm, Vc=1100 m/min result**

From Figures 8 to 16 different test cases chips are collected with respect their work-piece and cutting tool parameters. From the obtained experimental result, chips are continues chip since it is Aluminium material.

## 6. VALIDATION STUDY:

Validation studies of the all 9 different cases as shown in Table 6 have been carried out to measure chip width and chip thicknesses of obtained chips from work-piece for numerical simulation experimental validation purpose (Figure 17-29). Digital caliper is used to measure chip thickness and chip width.

In the Figure 17, chip width and chip thicknesses are measured from experimentally obtained chip which is from depth of cut 0.5 mm and spindle speed of 9000 rpm. Measurements have been taken on 10 different places to find average value from obtained chip for both chip width and thickness with manual calibration and neglected chip burr for measuring some points and in numerical simulation chip width is considered to be constant which is equal to 1mm. In simulation, this is represents *plane stress/strain thickness*. Values are

shown in Table 7. Same process has been carried out for remaining 8 cases which are shown in Tables from 8 to 15 and identified % error for chip width and thickness.

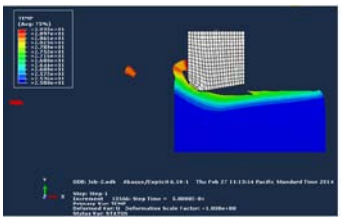

**Fig. 17 Chip width and chip thickness measurement for 0.5mm DOC, N= 9000 rpm**

**Table 7. Simulation and experimental result values for chip width and chip thickness for 0.5mm DOC and N=9000 rpm**

| Simulation result | | Experimental result | | Chip Width % error | Chip Thickness % error |
|---|---|---|---|---|---|
| Chip Width in mm | Chip thickness in mm | Chip Width in mm | Chip thickness in mm | ((Simulated chip width – Experimental chip width) / Simulated chip width)) | ((Simulated chip thick – Experimental chip thick) / Simulated chip thick)) |
| 1.00 | 0.15 | 0.85 | 0.07 | 15% | 54% |
| 1.00 | 0.15 | 0.86 | 0.06 | 14% | 60% |
| 1.00 | 0.15 | 0.79 | 0.08 | 21% | 47% |
| 1.00 | 0.15 | 0.82 | 0.07 | 18% | 54% |
| 1.00 | 0.15 | 0.88 | 0.07 | 12% | 54% |
| 1.00 | 0.15 | 0.82 | 0.08 | 18% | 47% |
| 1.00 | 0.15 | 0.68 | 0.08 | 32% | 47% |
| 1.00 | 0.15 | 0.75 | 0.07 | 25% | 54% |
| 1.00 | 0.15 | 0.88 | 0.09 | 12% | 40% |
| 1.00 | 0.15 | 0.90 | 0.07 | 10% | 54% |

**Table 8. Simulation and experimental result values for chip width and chip thickness for 0.5mm DOC and N=10000 rpm**

| Simulation result | | Experimental result | | Chip Width % error | Chip Thickness % error |
|---|---|---|---|---|---|
| Chip Width in mm | Chip thickness in mm | Chip Width in mm | Chip thickness in mm | ((Simulated chip width – Experimental chip width) / Simulated chip width)) | ((Simulated chip thick – Experimental chip thick) / Simulated chip thick)) |
| 1.00 | 0.15 | 0.93 | 0.12 | 7% | 20% |
| 1.00 | 0.15 | 0.71 | 0.07 | 29% | 54% |
| 1.00 | 0.15 | 0.62 | 0.10 | 38% | 34% |
| 1.00 | 0.15 | 0.95 | 0.08 | 5% | 47% |
| 1.00 | 0.15 | 0.88 | 0.07 | 12% | 54% |
| 1.00 | 0.15 | 0.92 | 0.09 | 8% | 40% |
| 1.00 | 0.15 | 0.99 | 0.10 | 1% | 34% |
| 1.00 | 0.15 | 0.91 | 0.09 | 9% | 40% |
| 1.00 | 0.15 | 0.90 | 0.07 | 10% | 54% |
| 1.00 | 0.15 | 0.92 | 0.07 | 8% | 54% |

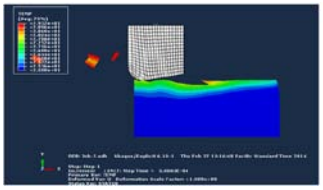

**Fig. 18 Chip width and chip thickness measurement for 0.5mm DOC, N= 10000 rpm**

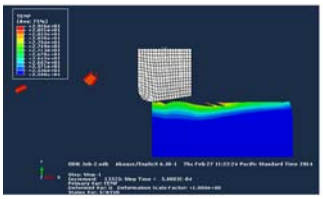

**Fig. 19 Chip width and chip thickness measurement for 0.5mm DOC, N= 11000 rpm**

**Table 9. Simulation and experimental result values for chip width and chip thickness for 0.5mm DOC and N=11000 rpm**

| Simulation result | | Experimental result | | Chip Width % error | Chip Thickness % error |
|---|---|---|---|---|---|
| Chip Width in mm | Chip thickness in mm | Chip Width in mm | Chip thickness in mm | ((Simulated chip width – Experimental chip width) / Simulated chip width)) | ((Simulated chip thick – Experimental chip thick) / Simulated chip thick)) |
| 1.00 | 0.15 | 0.95 | 0.06 | 5% | 60% |
| 1.00 | 0.15 | 0.75 | 0.05 | 25% | 67% |
| 1.00 | 0.15 | 0.83 | 0.08 | 17% | 47% |
| 1.00 | 0.15 | 0.96 | 0.09 | 4% | 40% |
| 1.00 | 0.15 | 0.88 | 0.07 | 12% | 54% |
| 1.00 | 0.15 | 0.69 | 0.08 | 31% | 47% |
| 1.00 | 0.15 | 0.91 | 0.08 | 9% | 47% |
| 1.00 | 0.15 | 0.81 | 0.07 | 19% | 54% |
| 1.00 | 0.15 | 0.89 | 0.08 | 11% | 47% |
| 1.00 | 0.15 | 0.81 | 0.08 | 19% | 47% |

**Table 10. Simulation and experimental result values for chip width and chip thickness for 1.0mm DOC and N=9000 rpm**

| Simulation result | | Experimental result | | Chip Width % error | Chip Thickness % error |
|---|---|---|---|---|---|
| Chip Width in mm | Chip thickness in mm | Chip Width in mm | Chip thickness in mm | ((Simulated chip width – Experimental chip width) / Simulated chip width)) | ((Simulated chip thick – Experimental chip thick) / Simulated chip thick)) |
| 1.00 | 0.15 | 1.23 | 0.11 | 23% | 27% |
| 1.00 | 0.15 | 1.10 | 0.11 | 10% | 27% |
| 1.00 | 0.15 | 1.37 | 0.16 | 37% | 7% |
| 1.00 | 0.15 | 1.11 | 0.13 | 11% | 13% |
| 1.00 | 0.15 | 1.29 | 0.12 | 29% | 20% |
| 1.00 | 0.15 | 1.13 | 0.11 | 13% | 27% |
| 1.00 | 0.15 | 1.44 | 0.15 | 44% | 0% |
| 1.00 | 0.15 | 1.40 | 0.11 | 40% | 27% |
| 1.00 | 0.15 | 1.36 | 0.14 | 36% | 7% |
| 1.00 | 0.15 | 1.46 | 0.13 | 46% | 13% |

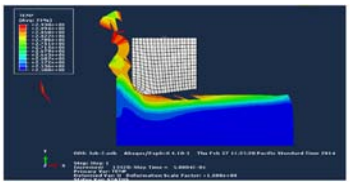

**Fig. 20 Chip width and chip thickness measurement for 1.0mm DOC, N= 9000 rpm**

**Table 11. Simulation and experimental result values for chip width and chip thickness for 1.0mm DOC and N=10000 rpm**

| Simulation result | | Experimental result | | Chip Width % error | Chip Thickness % error |
|---|---|---|---|---|---|
| Chip Width in mm | Chip thickness in mm | Chip Width in mm | Chip thickness in mm | ((Simulated chip width – Experimental chip width) / Simulated chip width)) | ((Simulated chip thick – Experimental chip thick) / Simulated chip thick)) |
| 1.00 | 0.15 | 1.44 | 0.21 | 44% | 39% |
| 1.00 | 0.15 | 1.43 | 0.20 | 43% | 33% |
| 1.00 | 0.15 | 1.43 | 0.18 | 43% | 19% |
| 1.00 | 0.15 | 1.50 | 0.29 | 50% | 92% |
| 1.00 | 0.15 | 1.50 | 0.25 | 50% | 66% |
| 1.00 | 0.15 | 1.37 | 0.21 | 37% | 39% |
| 1.00 | 0.15 | 1.47 | 0.21 | 47% | 39% |
| 1.00 | 0.15 | 1.43 | 0.20 | 43% | 33% |
| 1.00 | 0.15 | 1.48 | 0.21 | 48% | 39% |
| 1.00 | 0.15 | 1.49 | 0.21 | 49% | 39% |

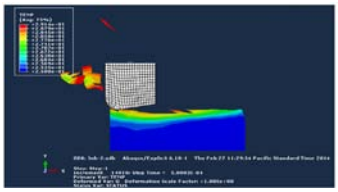

**Fig. 21 Chip width and chip thickness measurement for 1.0mm DOC, N= 10000 rpm**

**Table 12. Simulation and experimental result values for chip width and chip thickness for 1.0mm DOC and N=11000 rpm**

| Simulation result | | Experimental result | | Chip Width % error | Chip Thickness % error |
|---|---|---|---|---|---|
| Chip Width in mm | Chip thickness in mm | Chip Width in mm | Chip thickness in mm | ((Simulated chip width – Experimental chip width) / Simulated chip width)) | ((Simulated chip thick – Experimental chip thick) / Simulated chip thick)) |
| 1.00 | 0.15 | 1.44 | 0.21 | 44% | 39% |
| 1.00 | 0.15 | 1.18 | 0.19 | 18% | 26% |
| 1.00 | 0.15 | 1.11 | 0.18 | 11% | 19% |
| 1.00 | 0.15 | 1.50 | 0.16 | 50% | 6% |
| 1.00 | 0.15 | 1.35 | 0.15 | 35% | 1% |
| 1.00 | 0.15 | 1.49 | 0.17 | 49% | 13% |
| 1.00 | 0.15 | 1.43 | 0.23 | 43% | 52% |
| 1.00 | 0.15 | 1.35 | 0.21 | 35% | 39% |
| 1.00 | 0.15 | 1.42 | 0.21 | 42% | 39% |
| 1.00 | 0.15 | 1.45 | 0.19 | 45% | 26% |

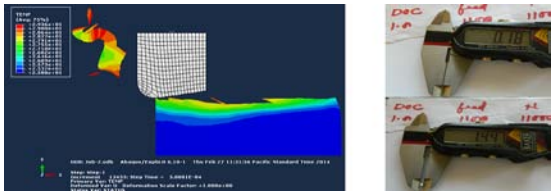

**Fig. 22 Chip width and chip thickness measurement for 1.0mm DOC, N= 11000 rpm**

**Table 13. Simulation and experimental result values for chip width and chip thickness for 1.5mm DOC and N=9000 rpm**

| Simulation result | | Experimental result | | Chip Width % error | Chip Thickness % error |
|---|---|---|---|---|---|
| Chip Width in mm | Chip thickness in mm | Chip Width in mm | Chip thickness in mm | ((Simulated chip width – Experimental chip width) / Simulated chip width)) | ((Simulated chip thick – Experimental chip thick) / Simulated chip thick)) |
| 1.00 | 0.15 | 1.53 | 0.16 | 53% | 6% |
| 1.00 | 0.15 | 1.62 | 0.13 | 62% | 14% |
| 1.00 | 0.15 | 1.37 | 0.18 | 37% | 19% |
| 1.00 | 0.15 | 1.55 | 0.16 | 55% | 6% |
| 1.00 | 0.15 | 1.35 | 0.18 | 35% | 19% |
| 1.00 | 0.15 | 1.30 | 0.24 | 30% | 59% |
| 1.00 | 0.15 | 1.48 | 0.18 | 48% | 19% |
| 1.00 | 0.15 | 1.49 | 0.17 | 49% | 13% |
| 1.00 | 0.15 | 1.51 | 0.18 | 51% | 19% |
| 1.00 | 0.15 | 1.30 | 0.22 | 30% | 46% |

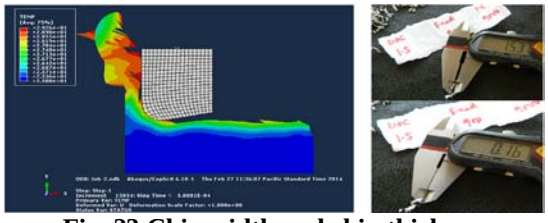

**Fig. 23 Chip width and chip thickness measurement for 1.5mm DOC, N= 9000 rpm**

**Table 14. Simulation and experimental result values for chip width and chip thickness for 1.5mm DOC and N=10000 rpm**

| Simulation result | | Experimental result | | Chip Width % error | Chip Thickness % error |
|---|---|---|---|---|---|
| Chip Width in mm | Chip thickness in mm | Chip Width in mm | Chip thickness in mm | ((Simulated chip width – Experimental chip width) / Simulated chip width)) | ((Simulated chip thick – Experimental chip thick) / Simulated chip thick)) |
| 1.00 | 0.15 | 1.41 | 0.22 | 41% | 46% |
| 1.00 | 0.15 | 1.37 | 0.21 | 37% | 39% |
| 1.00 | 0.15 | 1.50 | 0.16 | 50% | 6% |
| 1.00 | 0.15 | 1.28 | 0.16 | 28% | 6% |
| 1.00 | 0.15 | 1.32 | 0.20 | 32% | 33% |
| 1.00 | 0.15 | 1.43 | 0.21 | 43% | 39% |
| 1.00 | 0.15 | 1.41 | 0.22 | 41% | 46% |
| 1.00 | 0.15 | 1.47 | 0.25 | 47% | 66% |
| 1.00 | 0.15 | 1.51 | 0.23 | 51% | 52% |
| 1.00 | 0.15 | 1.48 | 0.21 | 48% | 39% |

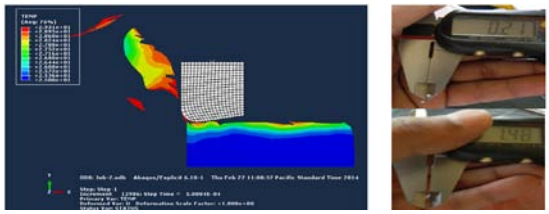

**Fig. 24 Chip width and chip thickness measurement for 1.5mm DOC, N= 10000 rpm**

**Table 15. Simulation and experimental result values for chip width and chip thickness for 1.5mm DOC and N=11000 rpm**

| Simulation result | | Experimental result | | Chip Width % error | Chip Thickness % error |
|---|---|---|---|---|---|
| Chip Width in mm | Chip thickness in mm | Chip Width in mm | Chip thickness in mm | ((Simulated chip width – Experimental chip width) / Simulated chip width)) | ((Simulated chip thick – Experimental chip thick) / Simulated chip thick)) |
| 1.00 | 0.25 | 1.59 | 0.28 | 59% | 12% |
| 1.00 | 0.25 | 1.65 | 0.24 | 65% | 4% |
| 1.00 | 0.25 | 1.31 | 0.20 | 31% | 20% |
| 1.00 | 0.25 | 1.66 | 0.26 | 66% | 4% |
| 1.00 | 0.25 | 1.24 | 0.17 | 24% | 32% |
| 1.00 | 0.25 | 1.59 | 0.24 | 59% | 4% |
| 1.00 | 0.25 | 1.68 | 0.27 | 68% | 8% |
| 1.00 | 0.25 | 1.56 | 0.28 | 56% | 12% |
| 1.00 | 0.25 | 1.47 | 0.24 | 47% | 4% |
| 1.00 | 0.25 | 1.48 | 0.22 | 48% | 12% |

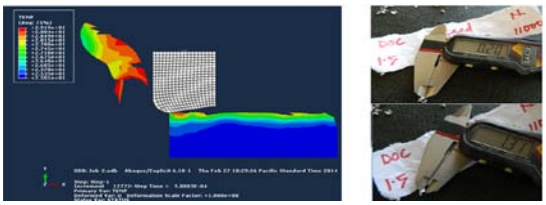

**Fig. 25 Chip width and chip thickness measurement for 1.5mm DOC, N= 11000 rpm**

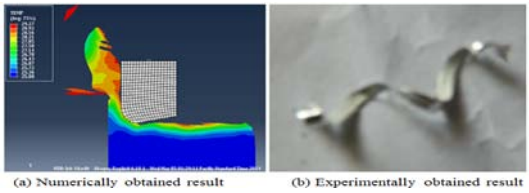


**Fig. 26 Comparison of chip geometries of N=9000 rpm and Depth of cut = 1.5 mm. (a) Simulated result (b) Experimental result**

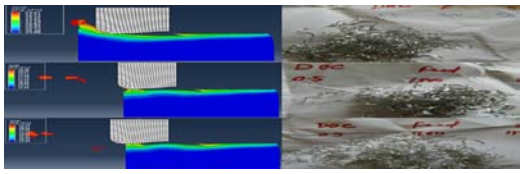

**Fig. 27 Chip morphology comparison between FEA vs Experimental of N =9000, 10000, 11000rpm respectively DOC= 0.5mm**

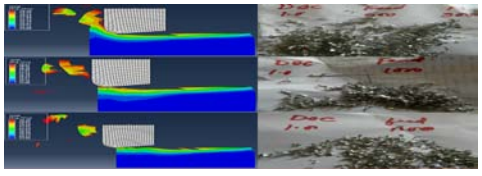

**Fig. 28 Chip morphology comparison between FEA vs Experimental of N =9000, 10000, 11000rpm respectively DOC= 1.0mm**

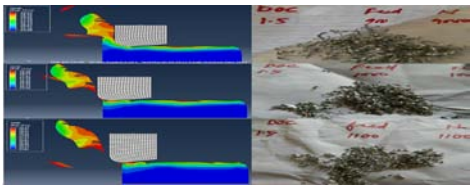

**Fig. 29 Chip morphology comparison between FEA vs Experimental of N =9000, 10000, 11000rpm respectively DOC= 1.5mm**

## 7. RESULTS AND DISCUSSIONS:

Figure 26, illustrates the comparison of chip morphology from ABAQUS simulated result to the experimental result. The serrated chip formation processes obtained from simulation are shown on the left Figure 26 (a). Experimental collected data from literatures are shown on the right Figure 26 (b). It is seen from the Figure 26 that both simulation and experiment give a continuous chip for material Al2024-T3 work piece.

Simulated chip morphology is compared with published data for different cutting speed, depth of cut, different spindle speed and of course different cutting speed but tool rake angle fixed to validates the proposed model. Throughout the simulation, the cutting tool Tungsten carbide tool with rake angle = 0°, clearance angle = +10° and tool nose radius of 0.8mm is used.

From table 16, it is indicate that % difference between FEA and experimental result validation for chip width is found to be in the range of 1-37%, which is good range and similarly for chip thickness, it is indicate the % difference between FEA and experimental result is found to be in the range of 0-40% which is also good range due to manual calibration for both chip thickness and chip width measurement. From all above results it is concluded that, numerical simulation software is reliable tool to predict chip morphology study. It is always agreed that, experimental result will not be 100% accuracy due to machine capability and manual calibration. It has been demonstrated that the ALE simulation approach presented in this work with adaptive meshing definitely results better predictions for chip morphology and chip formation.

**Table 16. Comparison table between FEA result and experiment result**

| Case no | Depth of cut in mm | Spindle speed in rpm | Rake angle in ° | FEA Width in mm | FEA thickness in mm | Exp Width in mm | Exp. Thickness in mm | Difference % between FEA and Exp for width | Difference % between FEA and Exp for thickness |
|---|---|---|---|---|---|---|---|---|---|
| 1 | 0.5 | 9000 | 0° | 1.00 | 0.15 | 0.90 | 0.07 | 10% | 40% |
| 2 | 0.5 | 10000 | 0° | 1.00 | 0.15 | 0.99 | 0.10 | 1% | 20% |
| 3 | 0.5 | 11000 | 0° | 1.00 | 0.15 | 0.96 | 0.09 | 4% | 40% |
| 4 | 1.00 | 9000 | 0° | 1.00 | 0.15 | 1.10 | 0.11 | 10% | 0% |
| 5 | 1.00 | 10000 | 0° | 1.00 | 0.15 | 1.37 | 0.21 | 37% | 19% |
| 6 | 1.00 | 11000 | 0° | 1.00 | 0.15 | 1.11 | 0.18 | 11% | 1% |
| 7 | 1.5 | 9000 | 0° | 1.00 | 0.15 | 1.30 | 0.22 | 30% | 6% |
| 8 | 1.5 | 10000 | 0° | 1.00 | 0.15 | 1.28 | 0.16 | 28% | 6% |
| 9 | 1.5 | 11000 | 0° | 1.00 | 0.25 | 1.24 | 0.17 | 24% | 4% |

## 8. CONCLUSIONS:

In this study, a thermo-mechanical numerical simulation model of plane-strain orthogonal metal cutting condition with continuous chip formulation is presented using the Finite Element Method software ABAQUS/Explicit. The developed model has proved to be able to predict chip morphology in a work piece that undergoes a typical high speed machining machine operation. That being said, numerical simulation for measuring chip width and chip thickness comparing with experimental result is found to be good. Predictions presented in this work also justify that the FE simulation technique used for orthogonal cutting process is an accurate and doable analysis as long as flow stress behavior of the work material obtained realistically and friction at the chip-tool interface is modeled correctly.

## 9. REFERENCES


[1] Deshayes L., Mabrouki T., Ivester R., Rigal J-F., *Serrated Chip Morphology and Comparison with Finite Element Simulations*, ASME IMECE04. November 13-20, 2004, USA, 2004.

[2] Özel T., *The influence of friction models on finite element simulations of machining*, International Journal of Machine Tools and Manufacture, 46, pp. 518-530, 2006.

[3] Zouhar J., Piska M., *Modelling the orthogonal machining process using cutting tools with deferent geometry*, MM Science Journal, 25-28, 2008.

[4] Shih A., *Finite Element Analysis of Orthogonal Metal Cutting Mechanics*, Int. J. Mach. Tools Manufact., Vol. 36, Issue 2, pp. 255-273, 1996.

[5] Shih A., *Finite Element Analysis of the Rake Angle Effects in Orthogonal Metal Cutting*, Int. J. Mech. Sci., Vol. 38, Issue 1, pp. 1-17, 1996.

[6] Kalhori V., *Modelling and Simulation of Mechanical Cutting*, Unpublished doctoral thesis, Luleå University of Technology, Luleå, Sweden, 2001.

[7] Stevenson M.G., Wrigt P.K., Chow, J.G., *Further Development in Applying the Finite Element Method to the Calculation of Temperature Distribution in Machining and Comparison with Experiment*, Journal of Engineering for Industry, 1983.

[8] Iwata K., Osakada K., Terasaka, Y., *Process Modeling of Orthogonal Cutting by the Rigid Plastic Finite Element Method*, Journal of Engineering Materials and Technology, 1984.

[9] Ueda K., Manabe, K., *Chip Formation in Microcutting of an Amorphous Metal*, Annals of CIRP, 1992.